Combined Effects of Grain Size Refinement and Dynamic Precipitation on Mechanical Properties of a New Magnesium Alloy

M.W. Vaughan, J.M. Seitz, R. Eifler, H.J. Maier, and I. Karaman

Abstract

Two well-known methods for enhancing the strength and controlling the anisotropy in magnesium alloys are precipitation hardening and grain size refinement. In this study, both methods are combined in an attempt to achieve optimal strengthening and anisotropy control: this was done via severe plastic deformation using Equal Channel Angular Processing (ECAP) of a precipitation hardenable magnesium alloy, Mg–6Zn–0.6Zr–0.4Ag–0.2Ca (wt%), within the temperature range of 125–200 °C. ECAP specimens were processed along different routes, where mechanically several of the ECAP samples show ultra-high strength levels approaching 400 MPa. The roles of grain size, texture, and precipitate morphology on mechanical properties are systematically investigated. It is shown here that the resulting microstructures generally show a refined grain size around 500 nm with a complex distribution of Mg-Zn enriched precipitates, which via ECAP either dynamically precipitate or are redistributed from the starting condition.

Keywords

Magnesium • Dynamic precipitation • Grain refinement • ECAP

Introduction

Magnesium alloys are prime candidates for weight sensitive applications due to their low density and high specific strength, and have thus been utilized extensively in the electronics industry and in the transportation industry for weight-critical applications [1–3]. Currently, several challenges facing Mg alloys are their limited formability, low mechanical strength, and high anisotropy at room temperature [2, 4]. A potential avenue for improving the mechanical strength of Mg, reducing anisotropy, and enhancing formability is via grain size refinement [4–6]. In addition, precipitation hardening has also been shown to effectively enhance strength and reduce anisotropy in Mg alloys [2, 3]. These two methods for mechanical and formability improvement in Mg can be potentially combined and optimized via equal channel angular processing (ECAP) for a given precipitation hardenable Mg alloy.

In general, a fine grain size enhances the strength of magnesium alloys according to the Hall-Petch relationship, where magnesium alloys have shown a considerably higher Hall-Petch coefficient than Al alloys [2]. To make the most of the Hall-Petch relationship, an ultrafine grain size (i.e. <1 μm) would be ideal [4]. An added advantage of a refined grain size is reduction of twinning activity [7, 8], thereby enhancing formability as twinning is often associated strain hardening and localization, followed by void nucleation and failure [8]. Razavi et al. successfully refined the grain size to ~0.35 μm via ECAP of the Mg-3Al-1Zn alloy (AZ31), obtaining a UTS over 400 MPa and a ductility approaching 15% [4]. Remarkably, ductility here was only slightly below the initial condition of ~18%, where the grain size was much larger (~33 μm) [4]. Evidently, grain refinement in

M.W. Vaughan (✉) · I. Karaman
Department of Materials Science and Engineering, Texas A&M University, College Station, TX, USA
e-mail: mattallicore@tamu.edu

J.M. Seitz · R. Eifler · H.J. Maier
Institut Für Werkstoffkunde (IW), Leibniz Universität Hannover, An der Universität 2, 30823 Hannover, Germany

K.N. Solanki et al. (eds.), *Magnesium Technology 2017*,
The Minerals, Metals & Materials Series, DOI 10.1007/978-3-319-52392-7_10

Mg can be advantageous for both strength and formability enhancement. Generally, to achieve an ultrafine grain size via ECAP, a multi-temperature step-down method is utilized, where grain size is refined further by gradually lowering the processing temperature in between passes for a given route [4–6]. In addition to strengthening via grain refinement, ECAP is also beneficial for controlling the crystallographic texture by reorienting the basal poles, and thus is capable of improving formability in Mg alloys by weakening the strong textures of wrought Mg products [4, 5].

Whereas grain refinement generally occurs via wrought processing, the effect of precipitation hardening on strength in Mg alloys typically requires aging the material after wrought processing [1]. Recently, Dogan et al. showed that a large amount of dynamic precipitation occurs during ECAP of AZ31 at low temperatures (150 °C) [9]. This is remarkable since Mg alloys such as AZ31 and ZK60 are generally not considered to be precipitation hardenable, as they demonstrate a limited age hardening response [2]. The effect of dynamic precipitates on mechanical properties of Mg-ZK alloys remains scarce in the literature. Statically aged precipitates are more often discussed. Mendis et al. demonstrated that precipitation hardening can be achieved in the ZK60 alloy by alloying with trace additions of Ag and Ca; these particles serve as precipitate nucleation sites and thus allow for a higher number density of $MgZn_2$ precipitates to form during the aging process [2, 3]. Here, a peak aged condition with a bimodal grain size averaging ~8.5 μm, with UTS nearing 350 MPa and an elongation approaching 15%, was produced [2]. Generally speaking, during precipitation hardening material strength increases with increasing precipitate number density (and consequently simultaneous refinement) [2, 10].

In the current study, the effect of grain size refinement and dynamic precipitation (rather than static precipitation) during ECAP is investigated on a precipitation hardenable Mg-ZKQX alloy. Here, ECAP was implemented on a precipitation hardenable Mg alloy via a multi-temperature step-down approach within the temperature range of 125–200 °C. Ultrafine grain sizes were produced, with a dynamically precipitated high number density of second phases. The mechanical characteristics of the processed samples are discussed with respect to grain size, precipitate morphology, and texture.

Experimental Procedures

The magnesium alloy ZKQX6000 (Mg 92.8 wt%, Zn 6 wt%, Zr 0.6 wt%, Ag 0.4 wt%, Ca 0.2 wt%) was chosen for this study due to its favorability for precipitation hardening [2]. The alloy was initially manufactured by gravity die-casting, where the base material and alloying elements were obtained commercially. In producing the quinary alloy, the bulk alloying components were melted at 750 °C in a steel crucible and afterwards stirred for 30 min. Due to the strong reactivity of magnesium with air, melting and casting were conducted under a protective argon atmosphere. After casting, hot extrusion was conducted. Here, a direct extrusion operation was arranged in a 10 MN extruder with the extrusion die heated to 300 °C along with the ZKQX recipient, which was inserted into the extruder and pressed through the extrusion die with a profile velocity of 0.05 m min^{-1}. This process, with an extrusion ratio of 16, produced a final square cross-section of 27.5 × 27.5 mm^2 for the extruded billet.

After extrusion, the bulk material was segmented via wire electrical discharge machining (EDM) into billets ~150 mm in length. Next, the billets were homogenized at 350 °C for 48 h under argon before being water quenched. Finally, billets were machined down to a 25 × 25 mm^2 cross section prior to ECAP. In this study, three billets of ZKQX, called A3-1, A3-3, and A3-4 in the text, were ECAP deformed, and their mechanical behavior is investigated and compared with the initial homogenized condition, called As-Rec in the text (see Table 1). Note that the results for specimen A3-2 are not reported here as it failed during the ECAP due to insufficient applied back pressure.

Specimens were ECAP-deformed through a press with a 90° die with sharp corners (Fig. 1) along different routes and temperatures (Table 1). Here, route A represents no rotation of the billet along its extrusion axis with respect to the ECAP press between passes (Fig. 1). In contrast, route C represents a 180° rotation between passes. As an example, the route shown in Table 1 for A3-1 means that it was

Table 1 ECAP processing details and resultant grain sizes for the ZKQX billets discussed in this study

Designation	Processing route and temperature	Avg. grain size (μm)
As-Rec	As Received	10.6 ± 7.2
A3-1	2A @ 200 °C + 180° rotation + 2A @ 150 °C + 1C @ 125 °C	0.54 ± 0.39
A3-3	4C @ 200 °C + 180° rotation + 2A @ 150 °C + 1A @ 125 °C	0.51 ± 0.25
A3-4	4C @ 200 °C + 180° rotation + 2A @ 150 °C	0.92 ± 0.39

See text for further details

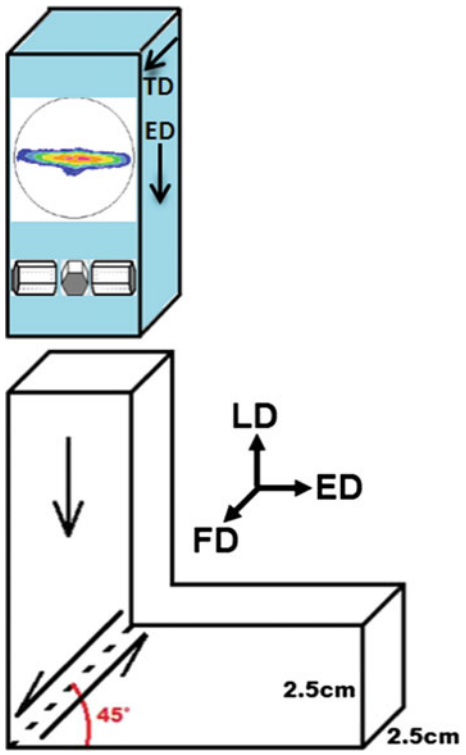

Fig. 1 Schematic of the ZKQX billets in blue with respect to the ECAP press utilized in this study. Prior ECAP—*TD* Transverse Direction, *ED* Extrusion Direction. Post ECAP—*FD* Flow Direction, *ED* Extrusion Direction, *LD* Longitudinal Direction. Basal poles are oriented 90° to the ED prior to ECAP

ECAP-deformed under two passes for route A at 200 °C, rotated 180° along its ED axis before going down to 150 °C for two more passes of route A. Finally, one pass of route C was conducted at 125 °C. Further details on ECAP routes with the current press can be found in ref. [11]; here, note that the routes chosen in this study are hybrid routes. For all ECAP experiments, extrusion rates of 4.5 mm min^{-1} were utilized at 200 and 150 °C, while at 125 °C the rate was reduced to 2.25 mm min^{-1} as a precaution. Also, back pressures of 20, 35, and 55 MPa were utilized for 200, 150, and 125 °C, respectively. Billets were heated for 30 min to temperature prior to each ECAP pass to homogenize the temperature throughout the sample.

The microstructure of the samples was examined using a Keyence VH-Z100 digital microscope and an FEI Quanta-600 SEM instrument. Three hundred grain diameters were individually measured via the ImageJ software package from multiple images, and their averages with standard deviations are reported in Table 1. Note that the average grain sizes reported here were cross-verified with the linear intercept method, which produced similar average grain sizes. The pole figures of the bulk samples were determined using a Bruker-AXS D8 X-ray diffractometer with Cu Ka (wavelength k = 0.15406 nm) radiation. Samples for microstructural characterization were cut from the mid-section of the deformed specimens from the flow plane. These samples were mechanically ground and subsequently polished with diamond paste to 0.1 µm. OM and SEM samples were etched via an acetic-picral acidic mixture (20 mL acetic acid, 3 g picric acid, 20 mL H_2O, 50 mL ethanol (95%)). Chemical analyses of the alloy precipitates prior ECAP was performed in a Cameca SX50 scanning electron microscope (SEM) equipped with four wavelength dispersive X-Ray spectrometers (WDS).

Flat, "dog-bone" tension specimens were cut via EDM along the extrusion direction (ED) and transverse direction (TD) for the As-Rec specimen, and along the flow and extrusion directions (FD and ED) for the ECAP specimens (Fig. 1). The gauge sections of the tensile specimens were $8 \times 3 \times 1.5$ mm^3. Compression samples of dimensions $4 \times 4 \times 8$ mm^3 were cut along each direction. Samples were cut with the gage sections located in the midsections of the ECAP billets to capture the mechanical performance along the fully worked regions [11]. Tension and compression tests were performed using a strain rate of 5×10^{-4}/s for all temperatures, using an MTS test frame with an MTS extensometer to record strain values.

Results

The as-extruded and homogenized microstructures and crystallographic textures are shown in Fig. 2. From the (0002) pole figure, the as-extruded microstructure demonstrates a typical extrusion texture with the c-axes aligning themselves normal to the ED (Fig. 2a). Here, notice long strands, or stringers, of second phases aligned along the ED. In addition, refined second particles are dispersed along the refined grains. To dissolve second phases into the matrix, the alloy was heat treated at 350 °C for 48 h; this condition is referred to as the As-Rec state (Fig. 2b), since it is the condition for all billets prior to ECAP. For the As-Rec condition, the sharp extrusion texture softened somewhat, although generally the c-axes remain normal to the ED. Notice also that the grains have grown and the refined secondary particles diffused into the Mg matrix. However, long stringers of second particles remain elongated along the ED. The elements composing these particles (white arrow in Fig. 2b) were evaluated using WDS as ~Zn-Mg-Ca enriched precipitates. The average grain size for the As-Rec condition was 10.6 µm, although it is worth mentioning that long stringer grains were also present and elongated along the ED (annotated in Fig. 2b).

Nominal mechanical responses for the As-Rec and ECAP-deformed specimens are included in Fig. 3. Note the ultra-high tensile strength levels in the A3-1 and A3-3 specimens along the FD. Representative microstructures for

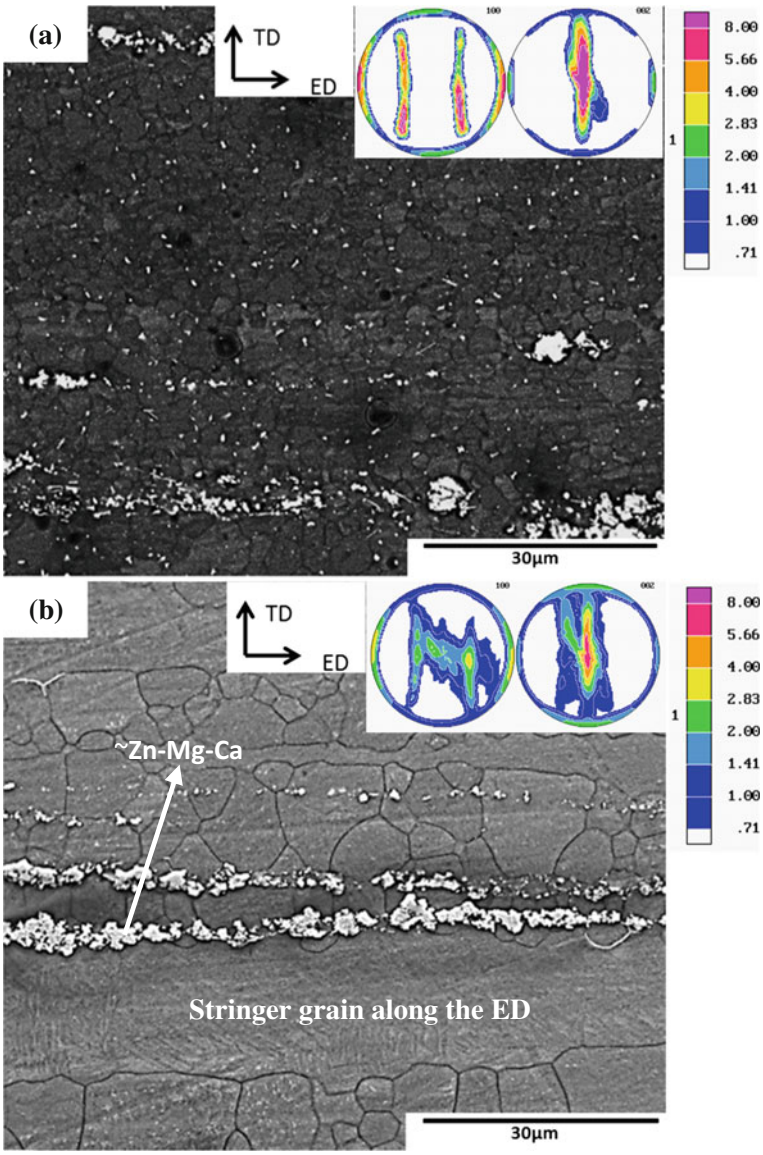

Fig. 2 Microstructure and (10-10) (*left*) and (0002) (*right*) pole figures of the **a** extruded and **b** As-Rec (i.e. extruded and homogenized at 350 °C for 48 h) ZKQX conditions

the A3-1, A3-3, and A3-4 billets post-ECAP are included in Fig. 4, where insets of the crystallographic textures are also included for the best mechanical results (A3-1 and A3-3). The corresponding grain sizes for the ECAP billets are shown in Table 1, where an ultrafine grain size was obtained for all three cases. Notice also the prevalence of second phases here more clearly seen in the BSE images of Fig. 4.

Discussion

In this study, ECAP successfully refined the grain size of a Mg-ZKQX alloy to ultrafine levels, while also dynamically precipitating a large amount of second phases from the original matrix. The role of precipitation, grain size, and texture in relation to mechanical properties are discussed in this section for the different conditions.

In the As-Rec condition, the second phases and grains are elongated along the ED (Fig. 2b), and tensile strength and ductility along the ED is much higher when compared to the TD (Fig. 3a). When analyzing the microstructure after failure along these specimens, it was found that failure occurred along the interfaces between the secondary Zn-Mg-Ca particles and grains during TD loading (Fig. 5b). However, during ED loading the precipitate stringers act as crack barriers (see crack annotated in white in Fig. 5a), reinforcing the surrounding Mg matrix. Thus, tensile failure occurred when the loading direction (TD) was normal to the precipitate elongation direction (ED). It is worth mentioning that TD loading is not generally reported for extruded material

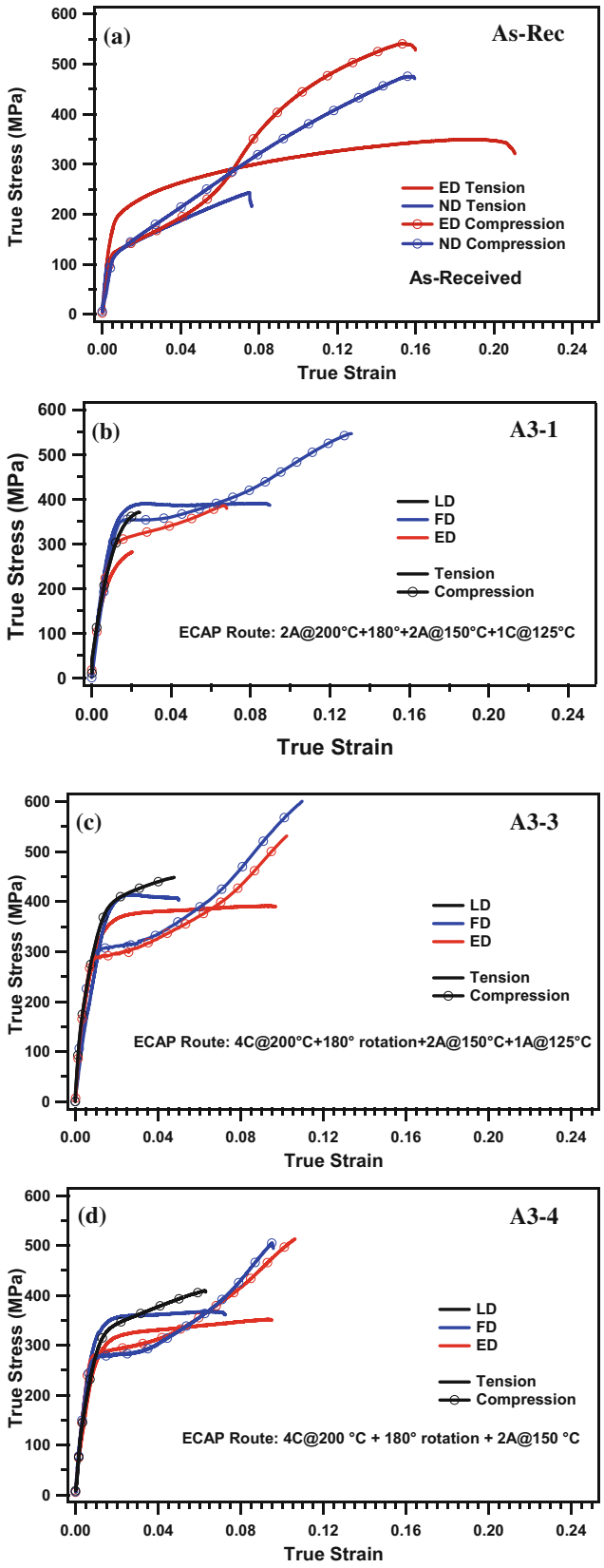

Fig. 3 True stress versus strain for tension and compression responses for **a** As-Rec, **b** A3-1, **c** A3-3, and **d** A3-4 specimens

[2, 3]. The As-Rec texture (Fig. 2b) primarily favors prismatic slip along the ED, which as a hard deformation mode could explain the higher yield strength for the ED in comparison to the TD. Compression tests (Fig. 3a) demonstrated high strain hardening characteristic of tensile twinning. The role of the precipitate-grain interface on failure is mentioned since it is may impact the mechanical behavior of the ECAP specimens.

ECAP of the As-Rec condition modifies precipitate morphology, grain size, and texture. Figure 6 captures a comparison of the Zn-Mg-Ca precipitate stringer morphologies, where precipitates are elongated along the ED initially (Fig. 2b and 6a). After one ECAP pass, they reorient towards the LD (Fig. 6b). Further processing modifies their arrangements as a function of the ECAP route (Fig. 6c–e). In addition to the precipitate stringers, Fig. 4 BSE images show ultrafine Mg-Zn rich precipitates dispersed along the ultrafine grains; in general these particles were observed throughout the ECAP specimens along DRX regions. Note that these precipitates were not observed in a few larger, non-deformed grains of the ECAP samples (e.g. in Fig. 7). Hence, they are considered precipitates which nucleated dynamically during the ECAP. Dynamic precipitation in Mg-ZK alloys is rarely mentioned in the literature. Dogan et al. recently showed that ECAP of AZ31, which like ZK60 is not considered a precipitation hardenable alloy, demonstrates dynamic precipitation also along the DRX regions at 150 °C [9]. In contrast, Mostaed et al. argued that ECAP of ZK60 at 150 °C refined the initial precipitate distribution, but they did not mention dynamic precipitation as a possible explanation [12]. In the present study, Figs. 4 and 6 indicate that both stringer precipitate reorientation and dynamic precipitation are occurring in the ZKQX alloy. The effects of these precipitates on failure are reserved for future studies.

Regarding grain size, the role of processing temperature is evident. Here, notice that at lower final processing temperatures, smaller grain sizes were produced (Table 1). This is expected from the multi-temperature step-down method [4, 6]. A remarkable yield strength increment from the As-Rec case (~190 MPa along the ED) to the A3-1, A3-3, and A3-4 cases (~380, ~395, and ~340 MPa, respectively, along the FD). In addition, a reduction in yield tension-compression anisotropy is most clearly evident after ECAP along the FD for A3-1 and the ED and FD for A3-4 (Fig. 3). Hall-Petch strengthening is therefore contributing to the enhanced mechanical properties of the ECAP specimens. However, note that along the ED and LD for the A3-1 case, poor strength and ductility were observed (Fig. 3b). One possible explanation could be delamination at the interfaces between the reoriented precipitate stringers and the matrix, similar to that observed in Fig. 5b for the As-Rec state. However, a detailed analysis of the fracture surface is needed

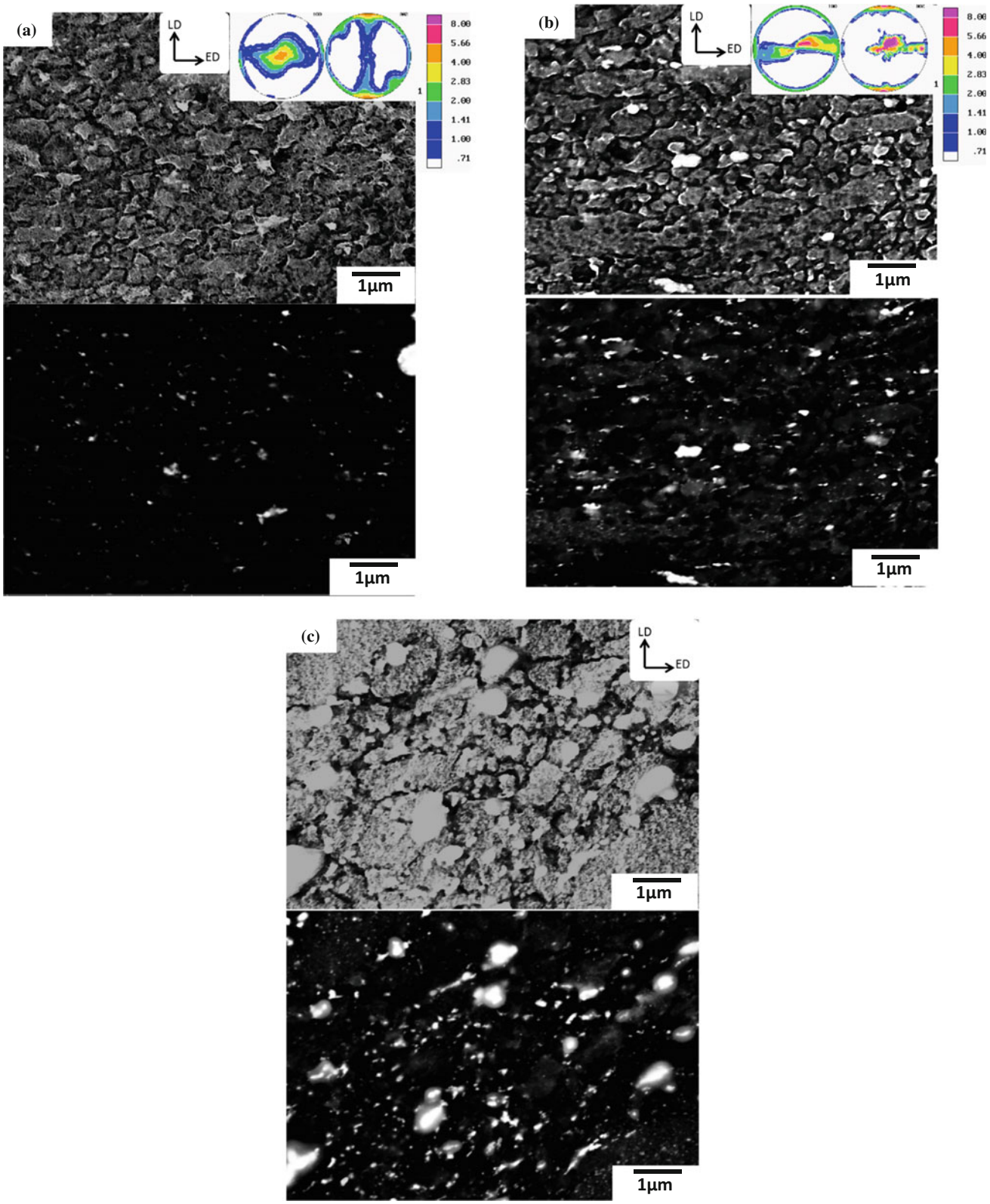

Fig. 4 SEM and BSE from the FD plane for the following: **a** A3-1, **b** A3-3, and **c** A3-4, showing a refined grain size and secondary Zn-rich particles along these regions. Pole figures—*left* (10-10), *right* (0002), where the same scale shown in Fig. 2 is used

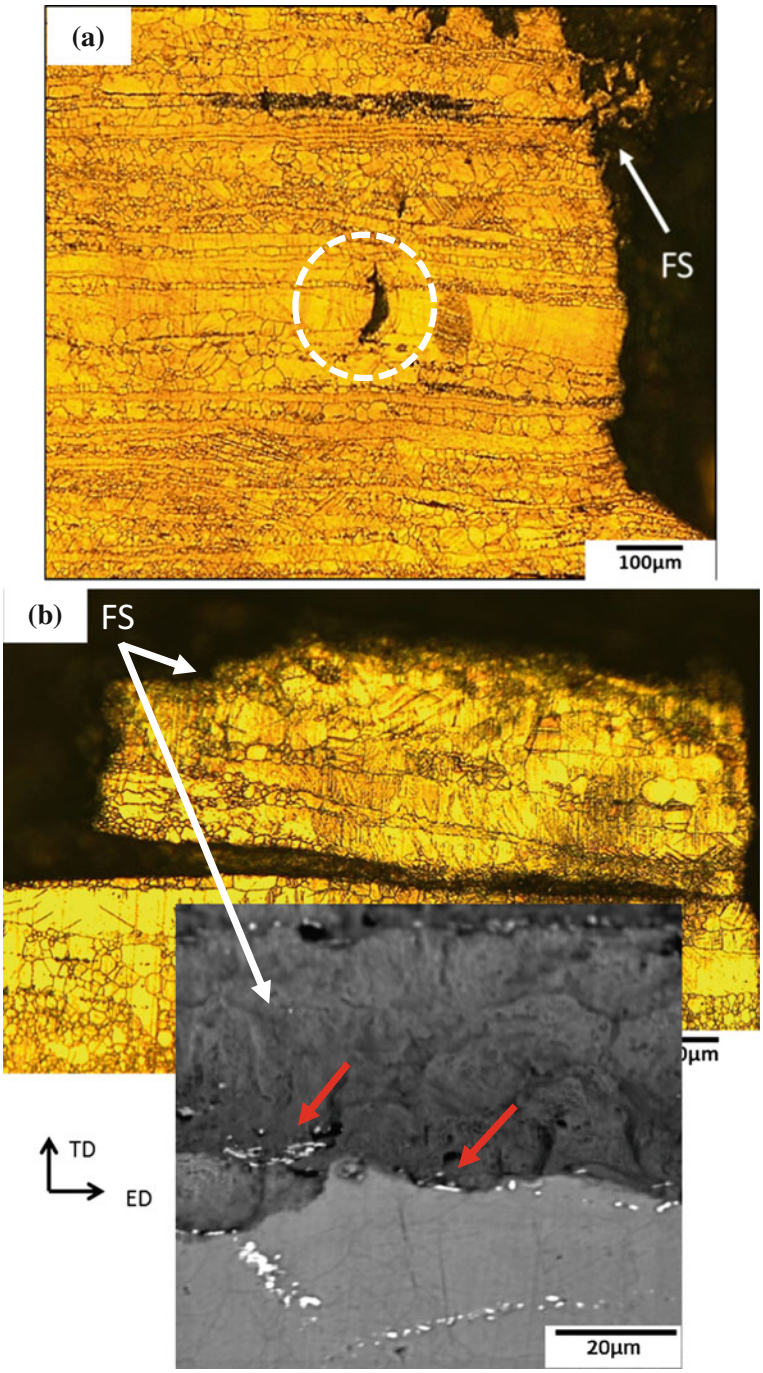

Fig. 5 As-Rec tension samples after failure when tested along the **a** ED and **b** TD. FS: fracture surface. See text for details

to prove this argument. The contributions of the dynamically precipitated Mg-Zn rich second phases on strength requires further investigation. It is possible that the second phases contribute to grain boundary pinning, resulting in enhanced strength and brittle failure.

Finally, the role of texture on mechanical properties is discussed, where an emphasis on the best mechanical responses is made for brevity. Note that in the A3-1 case, the basal poles are reoriented along the LD and ~45° to the LD (Fig. 4a). Tension along the FD shows respectable ductility (~10%) and an ultra-high UTS approaching 400 MPa (Fig. 3b). As the tensile axis is normal to the basal poles, prismatic slip is favored. Thus, the high strength levels with moderate ductility are a consequence of engineering the texture to favor prismatic slip, which with the ultrafine grain size allows for both high yield strength and favorable ductility. A similar finding was made in ref. [4]. In the A3-3 case, basal poles align both along the FD and LD axes. While tension along the FD exceeds 400 MPa in UTS, its ductility is limited (Fig. 3c). This may be a texture effect, as prismatic slip is not

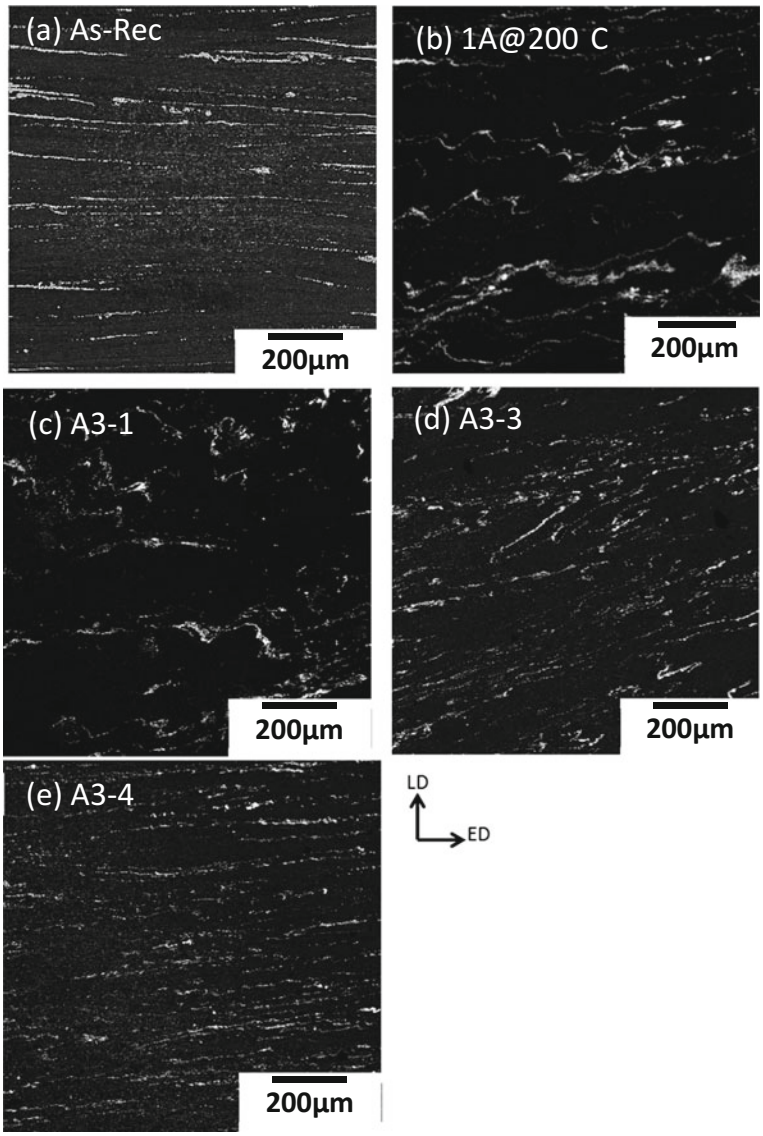

Fig. 6 **a**–**e** BSE images capturing the second phase Zn-Mg-Ca stringer morphology for different processing conditions, as annotated. Note that for **a** the TD rather than the LD is vertical

favorable since most c-axes align along the FD (Fig. 4b). Thus, c-axis extension (perhaps via tensile twinning or pyramidal <c + a> slip) should also occur while loading for the FD A3-3 case. In contrast, tension along the ED shows a higher ductility and a lower yield stress. Here, prismatic slip is more favorable as the basal poles are normal to the ED. The lower yield stress for the ED loading in comparison to the FD indicates that pyramidal slip has been activated along the FD, since pyramidal slip exhibits a higher CRSS than prismatic slip. An elaboration on the interaction effects between precipitates, grain size, and texture would be beneficial for expanding on the statements made here.

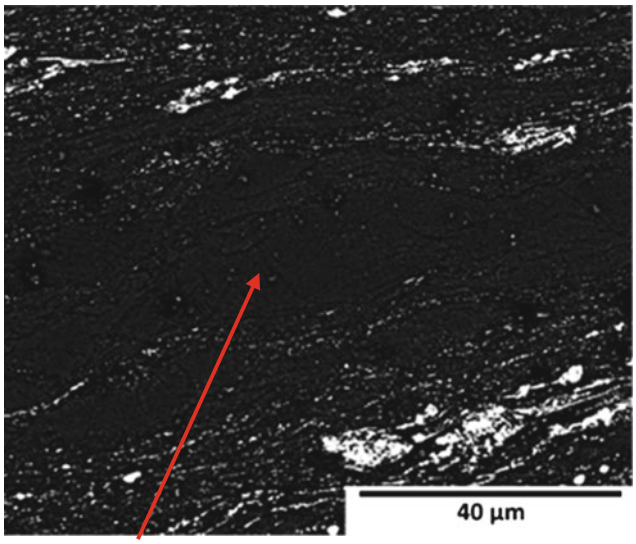

Fig. 7 BSE of a few large grains in the A3-3 ECAP specimen surrounded by DRX grain regions. The precipitates in white are clearly more prominent along the DRX grain regions

Conclusions

In this study, a Mg-ZK60 precipitation hardenable alloy containing trace additions of Ag and Ca was ECAP-deformed in an effort to enhance the mechanical strength by combining dynamic precipitation with Hall-Petch strengthening. Several main findings follow:

1. Ultrafine grain refinement was successfully achieved for the precipitation hardenable ZKQX Mg alloy, resulting in ultra-high strength levels (UTS ~400 MPa) for several orientations.
2. ECAP has a profound effect on precipitation for this alloy, both reorienting the initial precipitate stringers as well as dynamically precipitating an abundance of fine second phases along the DRX grain regions. The role of these phases on mechanical properties and failure requires further study.
3. Utilizing hybrid ECAP routes allowed for the development of a variety of textures for the ZKQX alloy. Combining grain refinement with texture control is shown to allow for both high strength with respectable ductility.

References

1. J.-F. Nie, Precipitation and hardening in magnesium alloys. Metall. Mat. Trans. A **43**, 3891–3939 (2012)
2. C.L. Mendis, K. Oh-ishi, Y. Kawamura, T. Honma, S. Kamado, K. Hono, Precipitation-hardenable Mg–2.4Zn–0.1Ag–0.1Ca–0.16Zr (at.%) wrought magnesium alloy. Acta Mater. **57**, 749–760 (2009)
3. C.L. Mendis, K. Oh-ishi, K. Hono, Enhanced age hardening in a Mg–2.4at.% Zn alloy by trace additions of Ag and Ca. Scripta Mater. **57**, 485–488 (2007)
4. S.M. Razavi, D.C. Foley, I. Karaman, K.T. Hartwig, O. Duygulu, L.J. Kecskes, S.N. Mathaudhu, V.H. Hammond, Effect of grain size on prismatic slip in Mg–3Al–1Zn alloy. Scripta Mater. **67**, 439–442 (2012)
5. E. Dogan, I. Karaman, G. Ayoub, G. Kridli, Reduction in tension–compression asymmetry via grain refinement and texture design in Mg–3Al–1Zn sheets. Mater. Sci. Eng. A **610**, 220–227 (2014)
6. D.C. Foley, M. Al-Maharbi, K.T. Hartwig, I. Karaman, L. J. Kecskes, S.N. Mathaudhu, Grain refinement vs. crystallographic texture: mechanical anisotropy in a magnesium alloy. Scripta Mater. **64**, 193–196 (2011)
7. M. Lentz, A. Behringer, C. Fahrenson, I. Beyerlein, W. Reimers, Grain size effects on primary, secondary, and tertiary twin development in Mg-4 wt pct Li (-1 wt pct Al) alloys. Metall. Mat. Trans. A **45**, 4737–4741 (2014)
8. M.R. Barnett, N. Stanford, P. Cizek, A. Beer, Z. Xuebin, Z. Keshavarz, Deformation mechanisms in Mg alloys and the challenge of extending room-temperature plasticity. JOM **61**, 19–24 (2009)
9. E. Dogan, S. Wang, M.W. Vaughan, I. Karaman, Dynamic precipitation in Mg-3Al-1Zn alloy during different plastic deformation modes. Acta Mater. **116**, 1–13 (2016)
10. J.D. Robson, C. Paa-Rai, The interaction of grain refinement and ageing in magnesium–zinc–zirconium (ZK) alloys. Acta Mater. **95**, 10–19 (2015)
11. R.E. Barber, T. Dudo, P.B. Yasskin, K.T. Hartwig, Product yield for ECAE processing. Scripta Mater. **51**, 373–377 (2004)
12. E. Mostaed, M. Hashempour, A. Fabrizi, D. Dellasega, M. Bestetti, F. Bonollo, M. Vedani, Microstructure, texture evolution, mechanical properties and corrosion behavior of ECAP processed ZK60 magnesium alloy for biodegradable applications. J. Mech. Behav. Biomed. Mater. **37**, 307–322 (2014)